Condensed Matter Physics, 2005, Vol. 8, No. 4(44), pp. 813–824

CONDENSED MATTER PHYSICS

Entropy of fermionic models on highly frustrated lattices

A.Honecker [1] , J.Richter [2]

[1] Technische Universität Braunschweig,
Institut für Theoretische Physik,
Mendelssohnstrasse 3,
38106 Braunschweig, Germany

[2] Institut für Theoretische Physik,
Otto-von-Guericke Universität Magdeburg,
39016 Magdeburg, Germany

Received July 20, 2005

Spinless fermions on highly frustrated lattices are characterized by the lowest single-particle band which is completely flat. Concrete realizations are provided by the sawtooth chain and the kagomé lattice. For these models a real-space picture is given in terms of localized states. Furthermore, we find a finite zero-temperature entropy for a suitable choice of the chemical potential. The entropy is computed numerically at finite temperature and one observes a strong cooling effect during adiabatic changes of the chemical potential. We argue that the localized states, the associated zero-temperature entropy as well as the large temperature variations carry over to the repulsive Hubbard model. The relation to flat-band ferromagnetism is also discussed briefly.

Key words: *flat band, localized states, frustrated lattice, spinless fermions, Hubbard model, magnetocaloric effect*

PACS: *71.10.Fd, 65.40.Gr, 75.30.Sg, 75.10.Jm*

1. Introduction

Frustrated quantum magnets exhibit a rich variety of semi-classically ordered and disordered ground states. This has been analyzed in some detail for two-dimensional models (see [1,2] for recent reviews). Interesting behaviour is also observed in a magnetic field, including plateaux in the zero-temperature magnetization curve and field-induced quantum phase transitions (compare [3,2,4] and references therein). A particularly intriguing phenomenon are non-interacting localized magnons which have recently been discovered at the saturation field of the spin-s XXZ model on highly frustrated lattices [3,2,4–6]. This gives rise to an enhanced magnetocaloric effect. Indeed, cooling rates around the saturation field in geometrically frustrated classical spin systems were predicted [7] to be up to several orders of magnitude bigger than in non-frustrated spin models. Enhanced cooling rates have also been verified experimentally, namely for $Gd_3Ga_5O_{12}$, a hyper-kagomé lattice (see [8] and references therein), and the pyrochlore magnet $Gd_2Ti_2O_7$ [9]. Since these results suggest applications for efficient low-temperature magnetic refrigeration, the magnetocaloric properties of the corresponding quantum systems are currently under intense investigation [10–15].

With the aid of the Jordan-Wigner transformation (see e.g. Chapter 1 of [16]), $s = 1/2$ XXZ chains can be mapped to spinless fermions. These are generally interacting fermions, but the interaction is irrelevant at low densities for sufficiently dispersive bands such that the low-temperature magnetocaloric properties at the transition to saturation in some quantum spin chains can be understood in terms of free spinless fermions [10]. Although there is no such direct connection for flat bands or in higher dimensions, we may still expect that free spinless fermions capture relevant qualitative features. This motivates us to analyze low-energy properties of free spinless fermions on the sawtooth chain (section 3) and the kagomé lattice (section 4), after a brief summary of some basic equations in section 2. In section 5 we discuss implications for the Hubbard model on the same lattices and mention a relation to flat-band ferromagnetism [17–21].

2. Model and basic equations

A central quantity of this paper is the entropy S. It is given in terms of the partition function Z by[1]

$$S(T) = \frac{\partial}{\partial T} T \ln Z \,. \tag{1}$$

Furthermore, we will analyze free spinless fermions, whose Hamiltonian reads

$$H = \sum_{\langle i,j \rangle} t_{i,j} \left(\hat{c}_i^\dagger \hat{c}_j + \hat{c}_j^\dagger \hat{c}_i \right) + \mu \sum_{i=1}^{N} \hat{n}_i \,. \tag{2}$$

The first sum runs over the nearest-neighbor pairs $\langle i,j \rangle$ of a lattice with N sites. $\hat{c}_i^\dagger$ and $\hat{c}_i$ are fermion creation and annihilation operators at site i with anticommutation relations $\left\{ \hat{c}_i^\dagger, \hat{c}_j \right\} = \delta_{i,j}$, and $\hat{n}_i = \hat{c}_i^\dagger \hat{c}_i$ is the number operator at site i. The hopping parameter $t_{i,j} > 0$ corresponds to the exchange constant of an antiferromagnetic spin-s XXZ model, and the chemical potential μ to a magnetic field h along the z-axis (the sign of μ has been chosen positive in order to allow for a direct comparison with the XXZ model in a magnetic field). We denote the single-fermion energies of (2) by ε_k and note that this one-particle problem is equivalent to the one-magnon problem relative to the ferromagnetically polarized state of the spin-s XX model on the same lattice. Furthermore, the Hilbert space of spinless fermions on

[1] The Boltzmann constant will be set to unity throughout this paper $k_{\mathrm{B}} = 1$.

an N-site lattice is isomorphic to that of the $s = 1/2$ XXZ model on the same lattice. Nevertheless, the many-particle states are not equivalent. Apart from the different statistics, interactions are absent in the model of spinless fermions (2). The latter property makes it straightforward to derive the thermodynamics, which is a challenging problem for the XXZ model.

For a free Fermi-gas the grand partition function[2] is given by $Z = \prod_k \left(1 + \mathrm{e}^{-\varepsilon_k/T}\right)$. Substitution into (1) yields the entropy for a system of free fermions

$$S(T) = \sum_k \ln\left(1 + \mathrm{e}^{-\varepsilon_k/T}\right) + \frac{1}{T}\sum_k \frac{\varepsilon_k\, \mathrm{e}^{-\varepsilon_k/T}}{1 + \mathrm{e}^{-\varepsilon_k/T}}\,. \tag{3}$$

3. Sawtooth chain

The first model to be discussed is the sawtooth chain shown in figure 1. The one-particle problem for (2) on the sawtooth chain leads to a 2×2 matrix whose eigenvalues yield two bands of one-particle energies

$$\varepsilon_\pm(k) = t\,\cos(k) \pm \sqrt{t^2\,\cos^2(k) + 2\,t'^2\,\cos(k) + 2\,t'^2} + \mu\,. \tag{4}$$

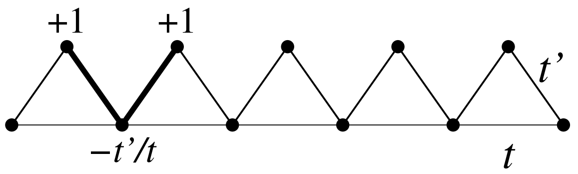

Figure 1. The sawtooth chain. The hopping parameter along the baseline is t, while along the diagonal directions it is t'. For $t' = \sqrt{2}\,t$ the one-particle states can be localized, as indicated by the bold line and the coefficients of the wave function (6) written next to the three associated sites.

When one chooses the hopping parameters along the diagonals $t' = \sqrt{2}\,t$ in terms of the hopping parameters along the baseline t, the one-particle energies become

$$\varepsilon_-(k) = -2\,t + \mu\,, \qquad \varepsilon_+(k) = 2\,t\,\left(1 + \cos(k)\right) + \mu\,. \tag{5}$$

Note that the lowest band $\varepsilon_-(k)$ is completely flat. The result (5) is equivalent to the one-magnon energies of an XX spin model on the sawtooth lattice [3]. Very similar results are also obtained for the Heisenberg model on this lattice (compare equation (33) of [10] for an explicit expression of the one-magnon energies for $s = 1/2$).

Now we will concentrate on the case $t' = \sqrt{2}\,t$ where the lowest band $\varepsilon_-(k)$ is completely flat. As in the XXZ model [3,4], it is possible to localize these one-particle states on the three sites indicated by the bold line (a "valley") in figure 1.

[2]The chemical potential μ is included in the definition of the one-particle energy ε_k for state k.

To be more precise, let us number the sites along the baseline by $2\,i$ and the ones at the top of the triangles by $2\,\mathrm{i}+1$. If we further denote the fermionic vacuum by $|0\rangle$, the localized wave functions are given by (up to normalization)

$$|l_{2\,i}\rangle = L^{\dagger}_{2\,i}\,|0\rangle\,, \qquad L^{\dagger}_{2\,i} = \hat{c}^{\dagger}_{2\,i-1} + \hat{c}^{\dagger}_{2\,i+1} - \sqrt{2}\,\hat{c}^{\dagger}_{2\,i}\,. \tag{6}$$

At $\mu = 2\,t$ we have $\varepsilon_{-}(k) = 0$. This implies a degeneracy of the ground states with $0 \leqslant n \leqslant 1/2$ due to the $2^{N/2}$ distinct ways to fill the zero-energy band. In this manner we have identified a zero-temperature entropy at $\mu = 2\,t$, $t' = \sqrt{2}\,t$

$$\frac{S(0)}{N} = \frac{\ln 2}{2} = 0.34657\ldots\,. \tag{7}$$

This corresponds to the zero-temperature entropy found in the Heisenberg model at the saturation field. However, the value in the latter case is smaller, namely $S(0)/N = 0.2406059\ldots$ [10–12]. That a larger value is obtained for free fermions can be understood as follows. Many-particle states can be constructed from localized one-particle states in different valleys. For spinless fermions it is possible to put one-particle states in neighbouring valleys. The corresponding two-particle state $L^{\dagger}_{2\,(i+1)}\,L^{\dagger}_{2\,i}\,|0\rangle$ is an exact eigenstate with energy $2\,\varepsilon_{-}$. However, in the XXZ model the energy of two localized magnons occupying neighbouring valleys is higher since they share a site [10,12]. The condition that two localized magnons may not occupy two neighboring valleys lowers the ground state degeneracy and hence the zero-temperature entropy of the XXZ model dereases as well.

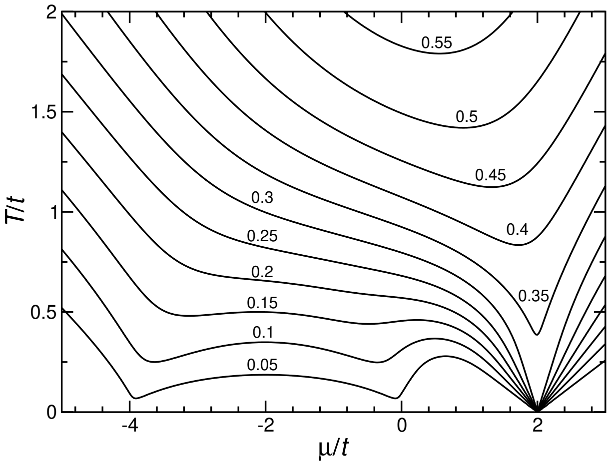

Figure 2. Lines of constant entropy for free spinless fermions on the sawtooth chain with $t' = \sqrt{2}\,t$. The value of the entropy per site $S(T)/N$ is indicated next to each line.

The entropy at finite temperature and with arbitrary μ can be evaluated from (3). One can either go to the thermodynamic limit and replace the sums by integrals. Alternatively, one can choose a large system size ($N = 2048$, for example) and evaluate the sums numerically. The latter has been performed to obtain figure 2 which is indistinguishable from the thermodynamic limit $N \to \infty$. The right half of this figure can be compared to figure 6(a) and figure 7 of [10] which show numerical results for the entropy of the $s = 1/2$ Heisenberg model in the h-T-plane. The following different low-temperature regions can be distinguished in figure 2:

(i) for $\mu > 2t$ both bands are empty and all excitations are gapped,

(ii) for $\mu = 2t$ the ground state is degenerate with the $T = 0$ entropy given in (7),

(iii) for $2t > \mu > 0$ the chemical potential is in the band gap between the lower band $\varepsilon_-(k)$ and the upper band $\varepsilon_+(k)$ such that excitations again have a gap,

(iv) for $0 \geqslant \mu \geqslant -4t$ the chemical potential is in the upper band $\varepsilon_+(k)$ and we have gapless low-energy excitations,

(v) for $\mu < -4t$ both bands are filled and all excitations are again gapped.

Now let us start at a small temperature T and change the chemical potential adiabatically. Such an adiabatic process keeps the entropy constant, therefore the temperature T has to change along the curves as in figure 2. If we approach the region (iv) either from region (iii) or region (v) we see that temperature drops as $\mu \to 0$ or $\mu \to -4t$. An even larger temperature drop is observed when we approach point (ii) either from region (i) or region (iii). This enhanced cooling is clearly due to the zero-temperature entropy (7) at $\mu = 2t$. In fact, if the entropy at the starting point is below this value, we theoretically approach $T \to 0$ as $\mu \to 2t$. The qualitative behavior is similar to that of the XXZ model on the sawtooth chain [10] (an interacting model) despite quantitative differences.

4. Kagomé lattice

In this section we discuss a two-dimensional lattice, the kagomé lattice shown in figure 3. Since a unit cell of this lattice contains three sites, the one-particle problem

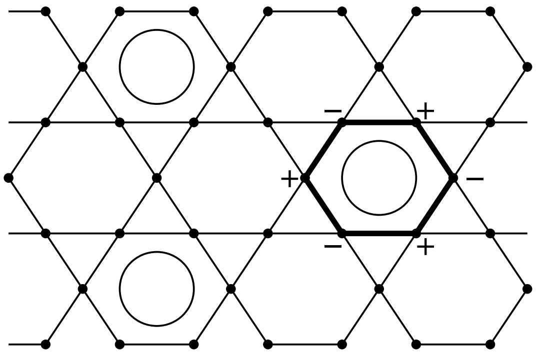

Figure 3. The kagomé lattice. The bold hexagon indicates a localized one-particle state, the signs in the corresponding wave function are written next to the six sites of this hexagon. Circles indicate the closest non-overlapping packing of localized one-particle states.

for the Hamiltonian (2) now leads to a 3×3 matrix whose eigenvalues yield three bands of one-particle energies

$$\begin{aligned}\varepsilon_0(k_x, k_y) &= \mu - 2t\,, \\ \varepsilon_\pm(k_x, k_y) &= \mu + t \pm t\sqrt{1 + 4\cos\left(\frac{k_x}{2}\right)\left(\cos\left(\frac{\sqrt{3}\,k_y}{2}\right) + \cos\left(\frac{k_x}{2}\right)\right)}\,. \end{aligned} \quad (8)$$

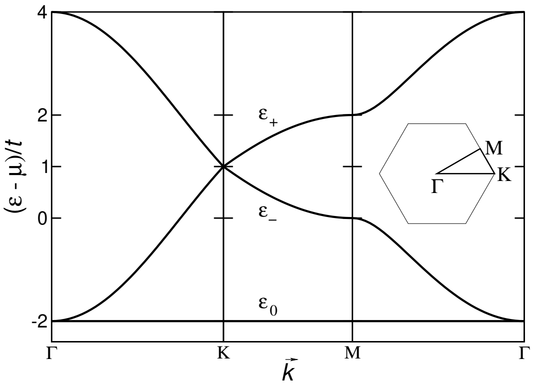

Figure 4. The three bands $\varepsilon_i(\vec{k})$ of single-particle energies for spinless fermions on the kagomé lattice along the path in the Brillouin zone shown in the inset. Note that $\varepsilon_0(\vec{k})$ is completely independent of $\vec{k}$.

Figure 4 shows these three one-particle bands along a path in the Brillouin zone. Note that the lowest band $\varepsilon_0(\vec{k})$ turns out to be completely flat. These results can be related to the known ones. Firstly, using a particle-hole transformation [17], the present problem maps to a tight-binding problem of electrons moving on the kagomé lattice (compare figure 4 e.g. with figure 1(b) of [22]). The one-magnon problem for the XXZ model on the kagomé lattice is another equivalent problem (see [3] and in particular figure 2.31 of [2], compare also equation (1) of [12]).

As in the XXZ model [3,2], it is again possible to localize these one-particle states in real space, namely on a hexagon, as indicated by the bold line in figure 3. If we number the sites around a hexagon h with $j = 1, \ldots, 6$, these localized wave functions can be written as (compare also figure 3 for the signs $(-1)^j$)

$$|l_h\rangle = L_h^\dagger\,|0\rangle\,, \qquad L_h^\dagger = \frac{1}{\sqrt{6}}\sum_{j=1}^{6}(-1)^j\,\hat{c}_{h,j}^\dagger\,. \quad (9)$$

The energy of the lowest band becomes $\varepsilon_0(\vec{k}) = 0$ at $\mu = 2t$. Consideration of all possible ways to fill this zero-energy band yields $2^{N/3}$ zero-energy excitations. For $\mu = 2t$ another one-particle energy vanishes, namely $\varepsilon_-(0,0) = 0$ (see figure 4). However, this occurs only at a single point $\vec{k} = \vec{0}$. Therefore, the additional contribution can be neglected in the thermodynamic limit $N \to \infty$. Hence, the zero-temperature entropy per site is at $\mu = 2t$

$$\frac{S(0)}{N} = \frac{\ln 2}{3} = 0.231049\ldots\,. \quad (10)$$

The XXZ model on the kagomé lattice also gives rise to a finite zero-temperature entropy at the saturation field [2,11,12]. A mapping of the configurations (9) to the exactly solved problem of hard hexagons [23,24] yields a lower bound $S(0)/N \geqslant 0.11108$ in this case [11,12]. On the one hand, one expects to find a lower entropy in the XXZ model than for spinless fermions, because the creation of localized magnons on two neighbouring hexagons costs no energy for free spinless fermions while localized magnons can be created for the XXZ model only on spatially separated hexagons. On the other hand, the situation remains more complicated than in one dimension because of additional topological effects. In fact, a class of many-magnon states has been found in the XXZ model which are independent of hard-hexagon configurations [12,14]. Therefore we believe that the precise value of the zero-temperature entropy at the saturation field of the $s = 1/2$ Heisenberg model on the kagomé lattice deserves further attention.

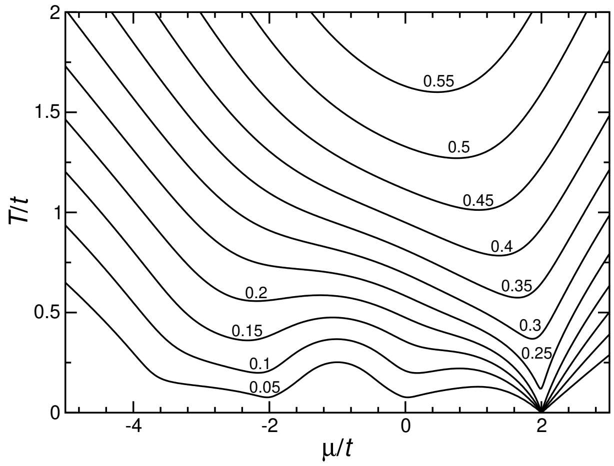

Figure 5. Lines of constant entropy for free spinless fermions on the kagomé lattice. The value of the entropy per site $S(T)/N$ is indicated next to each line.

Also for the kagomé lattice it is straightforward to obtain the entropy at finite temperature and with arbitrary μ from (3) and the single-particle energies (8). We have again evaluated the sums numerically on a large but finite lattice ($N = 10800$). The corresponding values of the entropy per site are shown in figure 5 and can be considered as representative for the thermodynamic limit. The following four low-temperature regions can be distinguished in figure 5:

(i) for $\mu > 2\,t$ all bands are empty and all excitations are gapped,

(ii) for $\mu = 2\,t$ the ground state is degenerate with the $T = 0$ entropy given in (10),

(iii) for $2\,t \geqslant \mu \geqslant -4\,t$ the chemical potential is in one of the bands $\varepsilon_{\pm}(\vec{k})$ and one has gapless low-energy excitations,

(iv) for $\mu < -4\,t$ all bands are filled and all excitations are again gapped.

Additional structures in region (iii) can be attributed to the features in the $T = 0$ single-particle density of states (compare Figure 4). Note that in contrast to the sawtooth chain, the kagomé lattice does not give rise to a gap for μ slightly below $2t$.

If we now change μ adiabatically, temperature drops considerably as $\mu \to 2\,t$. One can even reach $T = 0$ during an adiabatic process if the starting entropy is less than the $T = 0$ entropy (10) at $\mu = 2\,t$. Note the asymmetry of the curves in figure 5 around $\mu = 2\,t$: The dependence on μ is generally weaker in the gapless regime (iii) than in the gapped regime (i). We also observe a cooling effect as $\mu \to -4\,t$ from the gapped regime (iv), although unlike in figure 2 there is no pronounced minimum close to $\mu = -4\,t$.

5. Hubbard model and flat-band ferromagnetism

Now we will discuss the effect of interactions using the Hubbard model as an example. The fermions are assigned an additional spin index $\sigma =\uparrow, \downarrow$, and there is an on-site Coulomb repulsion $U > 0$ for fermions (electrons) with different spin:

$$H = \sum_{\sigma} \sum_{\langle i,j \rangle} t_{i,j} \left(\hat{c}^{\dagger}_{i,\sigma} \hat{c}_{j,\sigma} + \hat{c}^{\dagger}_{j,\sigma} \hat{c}_{i,\sigma} \right) + U \sum_{i=1}^{N} \hat{n}_{i,\uparrow} \hat{n}_{i,\downarrow} + \mu \sum_{\sigma} \sum_{i=1}^{N} \hat{n}_{i,\sigma} \,. \qquad (11)$$

The Coulomb repulsion is not effective for spin-polarized configurations (all σ equal). These configurations can be identified with spinless fermions. Conversely, each eigenstate of the spinless fermion Hamiltonian (2) yields a spin-polarized eigenstate of the Hubbard model (11). In particular the one-particle problem is identical in both models. The single-particle bands of the Hubbard model are simply twofold degenerate. Using the results from the previous sections, we can now establish a $T = 0$ entropy for the Hubbard model (11) for $U > 0$ and otherwise the same conditions which lead to $T = 0$ entropy for spinless fermions (2). A relation to flat-band ferromagnetism [17–21] is also evident.

Let us assume that the lowest single-particle band is completely flat, as we found for the sawtooth lattice (figure 1) at $t' = \sqrt{2}\,t$ and the kagomé lattice (figure 3). The corresponding states can be localized in real space as before; the creation operator of a local state $L^{\dagger}_{j,\sigma}$ just acquires an additional spin index. States localized at j_1, $j_2, \ldots$ with spins $\sigma_1, \sigma_2, \ldots$ can be created by repeated application of distinct creation operators

$$L^{\dagger}_{j_1,\sigma_1} L^{\dagger}_{j_2,\sigma_2} \cdots |0\rangle \,. \qquad (12)$$

These states are clearly eigenstates for any $j_1 \neq j_2$ if they are spin-polarized $\sigma_j = \sigma$. As long as the local states are created in spatially non-overlapping regions, the states (12) with $\sigma_1 \neq \sigma_2$ are also eigenstates with the same energy as the spin-polarized states. However, once the localization regions overlap, there are generally two electrons with a distinct spin at a site. The Coulomb repulsion in (11) raises the energy of such states by an amount of $\propto U$. Note that certain combinations where local states with different spins overlap must have the same energy as the spin-polarized states due to the $SU(2)$-symmetry of the Hamiltonian (11). However, if Coulomb repulsion is active, it will raise the energy of many-particle states in the lowest band.

Now choose μ such that the lowest band has zero energy $\varepsilon(\vec{k}) = 0$ ($\mu = 2\,t$ for the sawtooth chain and the kagomé lattice). The preceding discussion then yields a lower bound of the $T = 0$ entropy of the Hubbard model (11) in terms of spinless fermions (2): $S_{\mathrm{Hubbard}}(0) \geqslant S_{\mathrm{SF}}(0)$. The precise value of the entropy of the Hubbard model (11) is difficult to determine due to the additional zero-energy states which are not spin-polarized. In any case, in the Hubbard model adiabatic changes of μ will also give rise to large temperature variations.

Spatial overlaps of the individual local states are unavoidable at large filling fractions of the flat band. Spin-polarized states still have the lowest possible energy in this case while a non-polarized state is generally pushed higher in energy by Coulomb repulsion. This implies a phenomenon known as flat-band ferromagnetism [17–21]: In this region of densities, spin-polarized (i.e. ferromagnetic) configurations are preferred over non-magnetic configurations. To be more precise, let us consider the kagomé lattice. Using our conventions (11), the lowest band can be filled in a spin-polarized manner for $0 \leqslant n \leqslant 1/3$. On the other hand, local wave functions have to overlap for $n > 1/9$ (see figure 3). Slightly above the threshold $n = 1/9$, ferromagnetism can still be avoided by having an overlap only for localized states with equal spins. According to a detailed mathematical analysis [17], the ground state of the Hubbard model (11) is ferromagnetic for $1/6 < n \leqslant 1/3$.

6. Summary and outlook

In sections 3 and 4 we have examined spinless fermions on the sawtooth chain and the kagomé lattice. We found that the lowest single-particle band is completely flat for a particular choice of hopping parameters in the case of the sawtooth chain and without any fine-tuning for the kagomé lattice. These states can be localized in real space. Since the particles have zero energy at $\mu = 2\,t$, one finds a finite $T = 0$ entropy at this value of the chemical potential. This implies large adiabatic temperature variations when μ is changed adiabatically at finite temperature. At least on the single-particle level, the construction is completely analogous to the XXZ model on the same lattice. It can therefore be generalized to many other lattices for which localized magnons have been constructed [2–4,6], including in particular the pyrochlore lattice in three dimensions. We do not wish to speculate about possible experimental applications. Rather we regard these non-interacting models as an illustration of important qualitative features of spin models. First experimental investigations [8,9] of the magnetocaloric effect in highly frustrated magnets shows that they are indeed promising candidates for efficient low-temperature magnetic cooling.

The tuning of the chemical potential μ through a non-degenerate band-edge, i.e. an edge without flat directions, yields a second-order quantum phase transition. Spinless fermions thus provide a simple realization of the quantum critical scenario discussed in detail in [25,26].

In section 5 we have briefly commented on the Hubbard model where an on-site Coulomb repulsion U gives rise to interactions. However, this repulsion is not active for spin-polarized configurations. Therefore, the existence of a finite $T = 0$ entropy for a certain value of μ and consequently the large temperature variations when μ is tuned through this point carry over from spinless fermions to the Hubbard model. Nevertheless, both the $T = 0$ entropy and the cooling rate in the Hubbard model remain to be analyzed in more detail. In this context it is also intriguing to note that a finite $T = 0$ entropy arises in the Hubbard model under the same conditions which lead to flat-band ferromagnetism [17–21].

Acknowledgements

The present work was inspired by discussions and collaborations with H. Frahm and M.E. Zhitomirsky which are gratefully acknowledged.

References

1. Misguich G., Lhuillier C., Two-dimensional quantum antiferromagnets, p. 229–306. In: Frustrated Spin Systems, ed. Diep H.T. World Scientific, Singapore, 2004.
2. Richter J., Schulenburg J., Honecker A., Lect. Notes Phys., 2004, **645**, 85.
3. Schulenburg J. et al., Phys. Rev. Lett., 2002, **88**, 167207.
4. Richter J. et al., J. Phys.: Condens. Matter, 2004, **16**, S779.
5. Schnack J., Schmidt H.-J., Richter J., Schulenburg J., Eur. Phys. J. B, 2001, **24**, 475.
6. Richter J. Preprint arXiv:cond–mat/0503243, 2005.
7. Zhitomirsky M.E., Phys. Rev. B, 2003, **67**, 104421.
8. Zhitomirsky M.E., Golov A.I., Berkutov I.B., Petrenko O.A. Preprint, 2001, http://grendel.ph.man.ac.uk/Research/GGG1.pdf.
9. Sosin S.S. et al., Phys. Rev. B, 2005, **71**, 094413.
10. Zhitomirsky M.E., Honecker A., J. Stat. Mech.: Theor. Exp., 2004, 07012.
11. Derzhko O., Richter J., Phys. Rev. B, 2004, **70**, 104415.
12. Zhitomirsky M.E., Tsunetsugu H., Phys. Rev. B, 2004, **70**, 100403(R).
13. Schnack J. Preprint arXiv:cond–mat/0501625, 2005.
14. Zhitomirsky M.E., Tsunetsugu H. Preprint arXiv:cond–mat/0506327, 2005.
15. Honecker A., Wessel S. Preprint, 2005, http://www.tu-bs.de/˜honecker/papers/sces05.ps.gz.
16. Takahashi M. Thermodynamics of one-dimensional solvable models. Cambridge University Press, Cambridge, 1999.
17. Mielke A., J. Phys. A: Math. Gen., 1992, **25**, 4335.
18. Tasaki H., Phys. Rev. Lett., 1992, **69**, 1608.
19. Mielke A., Tasaki H., Commun. Math. Phys., 1993, **158**, 341.
20. Tasaki H., Progr. Theor. Phys., 1998, **99**, 489.
21. Nishino S., Goda M., Kusakabe K., J. Phys. Soc. Jpn., 2003, **72**, 2015.
22. Kimura T., Tamura H., Shiraishi K., Takayanagi H., Phys. Rev. B, 2002, **65**, 081307(R).
23. Baxter R.J., Tsang S.K., J. Phys. A: Math. Gen., 1980, **13**, 1023.
24. Baxter R.J., J. Phys. A: Math. Gen., 1980, **13**, L61.
25. Zhu L., Garst M., Rosch A., Si Q., Phys. Rev. Lett., 2003, **91**, 066404.
26. Garst M., Rosch A. Preprint arXiv:cond–mat/0506336, 2005.

Ентропія ферміонних моделей на сильно розвпорядкованих гратках

А.Гонекер [1] , Й.Ріхтер [2]

[1] Технічний університет Брауншвейга,
Інститут теоретичної фізики,
38106 Брауншвейг, Німеччина

[2] Інститут теоретичної фізики,
Університет Магдебурга ім. Отто фон Гюріке,
39016 Магдебург, Німеччина

Отримано 20 липня, 2005

Безспінові ферміони на сильно розвпорядкованих гратках характеризуються найнижчою одночастинковою зоною, яка є повністю плоскою. Конкретні реалізації зроблені за допомогою пилкоподібного ланцюжка та гратки Кагоме. Для цих моделей приведено картину в дійсному просторі в представленні локалізованих станів. Далі ми знаходимо скінчену ентропію при нульовій температурі для певного вибору хімічного потенціалу. Ентропія розраховується чисельно при скінченій температурі і спостерігається сильний ефект охолодження під час адіабатичних змін хімічного потенціалу. Ми аргументуємо, що локалізовані стани, відповідна ентропія при нульовій температурі як і сильні варіації температури переносяться на модель Габбарда з відштовхуванням. Коротко обговорюється також зв'язок із феромагнетизмом плоских зон.

Ключові слова: *плоска зона, локалізовані стани, розвпорядкована гратка, безспінові ферміони, модель Габбарда, магнетокалоричний ефект*

PACS: *71.10.Fd, 65.40.Gr, 75.30.Sg, 75.10.Jm*